Spectroscopy of high Rydberg states of highly charged ions and antiprotonic helium atoms

Hiroyuki A. Torii,[*1] Y. Morishita,[*2] Y. Yamazaki,[*1,*2] K. Komaki,[*1] K. Kuroki,[*1] R. Hutton,[*3] K. Ishii,[*4] K. Ando,[*2]
H. Masuda,[*5] M. Sekiguchi,[*6] M. Hori,[*7] E. Widmann,[*7] and R. S. Hayano[*7]
[*1] *Institute of Physics, University of Tokyo, Komaba Campus*
[*2] *Atomic Physics Laboratory, RIKEN*
[*3] *Department of Physics, University of Lund, Sweden*
[*4] *Department of Engineering Science, Kyoto University*
[*5] *Department of Industrial Chemistry, Tokyo Metropolitan University*
[*6] *Center for Nuclear Study, University of Tokyo, RIKEN Campus*
[*7] *Department of Physics, University of Tokyo, Hongo Campus*

We have performed fluorescence spectroscopy of high Rydberg states of highly charged ions (HCIs) extracted *in vacuum* using a microcapillary foil target. We identified photons emitted from ions with one electron in a high Rydberg state, for $\Delta n = 1$ transitions from $Q - 1 \leq n \leq Q + 3$ states in the VUV-visible-NIR light range. Time-resolved measurements clearly showed radiative cascade, and the initial population was deduced for the first time by our analysis which revealed that the electrons are preferentially transferred to states around $n \sim Q + 1$, in good agreement with the classical over-barrier model. Also, laser spectroscopy of antiprotonic helium atom is introduced in the latter section to give a hint to the similar time-variant method for the aim of mapping the initial population, which gives an important information of atomic capture process of antiprotons.

Spectroscopic methods such as observation of fluorescence light or measurements of laser resonance often work as powerful tools for the study of atomic structures and dynamics. Exotic atomic systems like Hollow Atoms and Antiprotonic Atoms are of much interest not only because of their peculiar structure with large quantum numbers but also because they give important information on the dynamic processes of electron transfer and atomic capture of exotic particles.

Spectroscopy of high Rydberg HCI

When a slow highly charged ion (HCI) approaches a metal surface, valence electrons in the metal start to be transferred to high-lying Rydberg states of the HCI at a critical distance, which is followed by subsequent electron transfers to lower states of the HCI when the HCI further approaches the surface. As a result, a "Hollow Atom" (HA) which has many electrons in outer shells and a few electrons in inner shells is formed above the surface. Although the formation of the above-surface HA is indirectly confirmed through measurements of the angular distribution of reflected ions under glancing angle of incidence[1)] or secondary electron yield during neutralization,[2)] no information on the electronic configurations of the HA have been available so far. This is because of the fact that the survival time of the HCI above the surface was inevitably limited to 10^{-13} s before the formed HA gets accelerated by its self-induced image and collide violently with the surface. To overcome the difficulty and in order to extract the formed HA *in vacuum*, we have developed a technique[3)] to use a capillary foil, a thin ($\sim 1\,\mu$m) Ni foil with many small straight holes with a diameter of *ca.* 100 nm. HCIs are injected along the capillary axis, and then some HCIs have a chance to transmit through the capillary, capture one of more electrons from the wall surface near the exit, escaping from hard crush with the wall by emerging from the capillary. This technique makes it possible for the first time to extract HCIs which have captured electrons in high-lying Rydberg states of the HCIs, and as a result, to study the initial stage of the neutralization process precisely.

The experiment was performed with 2.0 keV/u Ar^{Q+} ion beams (Q = 6–10) extracted from a 14.25 GHz HyperECR ion source at the Center for Nuclear Study, University of Tokyo. Figure 1 shows a schematic drawing of the experimental setup. The beam was first charge-state selected with an analyzing magnet, collimated to $1 \times 1\,\text{mm}^2$ in size with both a four-jaw slit system and a square aperture just in front of a

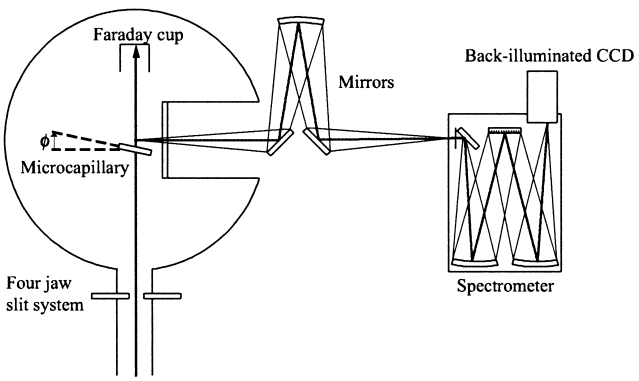

Fig. 1. Schematic drawing of the experimental setup.

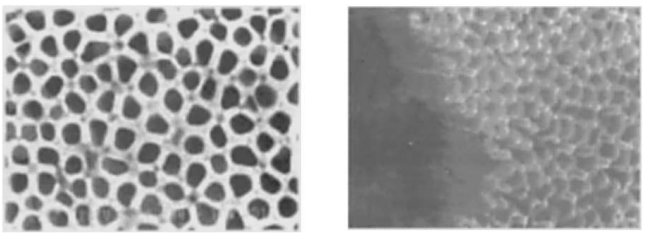

Fig. 2. Picture of microcapillary foil. Top view (left) and a side view (right) are shown.

Ni microcapillary target. The target chamber was evacuated to less than 10^{-8} Torr during the experiments. The microcapillary foil had a $\sim 1\,\mathrm{mm}^2$ effective size and a thickness of $\sim 700\,\mathrm{nm}$, with many straight holes of $\sim 100\,\mathrm{nm}$ diameter in a honeycomb-type structure (see Fig. 2). The position and orientation of the target were adjusted to maximize the transmitted beam current with an x–y–z–ϕ–θ manipulator, where ϕ and θ axes are parallel to z and x axes, respectively. Lifetime measurements can be performed by moving the target along y (*i.e.* the beam) direction. The distance of the position of the observation window from the target divided by the projectile velocity gives the time spent by the HA after its formation. The transmitted beam current was about 1–3% of the incident beam. Fluorescence photons emitted perpendicular to the beam trajectory (within the observation window determined by the entrance slit) were transferred to a Czerny-Turner type spectrometer with 1 to 1 imaging mirrors, and were detected with a back-illuminated CCD with a minimum resolution of $\sim 0.032\,\mathrm{nm}$ at 400 nm. We used both mercury and cadmium/neon hollow cathode lamps for the wavelength calibration. The relative efficiency of the detection system was calibrated with a standard deuteron lamp from 200 to 400 nm and with a tungsten lamp from 350 to 800 nm.

Figure 3 shows spectra for Ar^{Q+} ($6 \le Q \le 10$) incident ions with kinetic energy of 2.0 keV/u. Some lines are easily attributed to $\Delta n = 1$ transitions of the ions which have captured one electron in the capillary. The transition wavelengths can be well accounted for by assuming energy levels as those of hydrogenic. For example, in the case of the Ar^{8+} incident ion, transition wavelengths of Ar^{7+} from $1s^2 2s^2 2p^6 nl^1$ to $1s^2 2s^2 2p^6 (n-1)l'^1$ states are calculated to be 298, 434, 607, and 820 nm for n =8, 9, 10, and 11, respectively (k, l, m, and n in Fig. 3). Similarly, intense lines referred to as $a, b, ..., u$ in Fig. 3 can be attributed to $\Delta n = 1$ transitions from the initial states n, where $Q - 1 \le n \le Q + 3$.

The initial states to which the first electron transfer occurs shift to higher states when incident charges become larger, which can be accounted for as follows. According to the classical over-barrier model (COBM),[4] when slow highly charged ions approach a metal surface, the first electron transfer takes place to a $n_c \sim Q/[2W(1 + (Q - 0.5)/(8Q)^{1/2})]^{1/2}$ state of the incident ions (in the atomic units), where W is a work-function of the surface. By adopting a reasonable value of 0.2 a.u. for W, n_c can be approximated to be $Q + 1$.

We have also performed lifetime measurement for the identified lines by moving the position of the target along the beam axis, as was explained before. It was found that the apparent lifetime of the states were significantly longer (by factor nearly 2) than their intrinsic lifetime calculated using the dipole moments of the hydrogen-like Rydberg atom. Since the assumption of hydrogenic dipole moments should be valid enough for the system of small core and only one electron in the high Rydberg state, the enhanced lifetime gives an evidence for feeding cascade from upper states. Systematic studies were performed for single electron capture of Ar^{7+} incidence, *i.e.* for $\mathrm{Ar}^{7+}e^-$ Rydberg atom, and the decay curves of the designated transitions were compared with a cascade calculation. The result of the analysis revealed that the electron is captured to states with a principal quantum number very close to that predicted by the classical over-barrier model[4] and that the n distribution is rather sharp. This gives the first direct proof of COBM for the electron transfer to HCI from metallic surfaces.

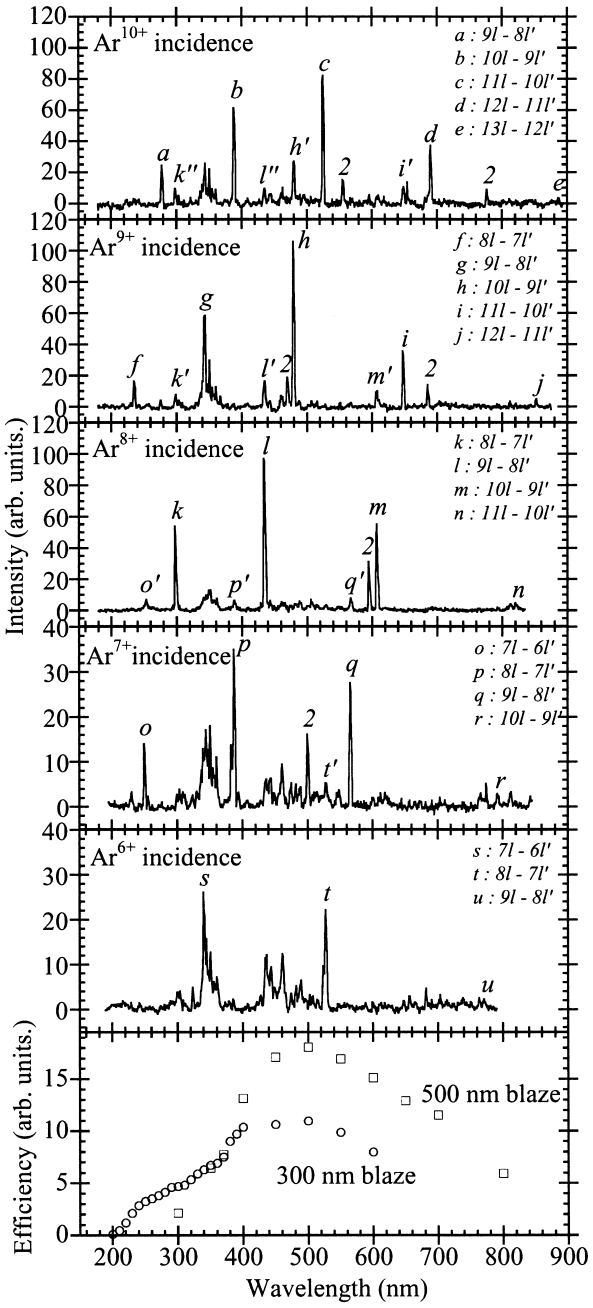

Fig. 3. Observed spectra for Ar^{Q+} ($6 \le Q \le 10$) incident ions and relative efficiency curves of the detection system.

It is noted that the lines observed for Ar^{Q+} incident ions can also be observed at the same wavelengths for $Ar^{(Q+1)+}$ incident ions, which is labeled by primed letters like k' in Fig. 3. This indicates that $Ar^{(Q+1)+}$ ion has captured two or three electrons in the capillary, and deexcited through radiative or Auger transitions leaving one electron in its high Rydberg states. Further, experiments with higher resolution have shown that (1) electrons are preferentially transferred around Yrast states, *i.e.*, the states with largest angular momentum ($l \sim n-1$) states, and (2) the angular momentum distribution were quite different between Ar^{8+} and the other Ar^{Q+} incident ions, which indicates that the core polarizability of the incident ions may have a large influence on the angular momentum distribution. A more detailed explanation will be given in a forthcoming publication.[5)]

Spectroscopy of antiprotonic helium atoms

Antiprotons will annihilate immediately after nuclear capture in media, but only when they stop in helium media, 3% of them show enormous longevity. This unique phenomenon is understood by the formation of so-called "antiprotonic helium atoms" ($(\overline{p}He^+)^0 \equiv \overline{p}e^-He^{++}$; see Fig. 4), and these exotic atoms have been extensively studied by the PS205 collaboration using the LEAR (Low Energy Antiproton Ring) facility, then succeeded by ASACUSA collaboration[6)] at AD (Antiproton Decelerator) at CERN, Geneva.

Metastable antiprotonic helium atom is a highly excited Rydberg system with typical quantum numbers $n \sim n_0 \equiv \sqrt{M^*/m_e} \approx 38$ (where M^* is the reduced mass between antiproton and helium nucleus, while m_e is the electron mass) and $l \lesssim n-1$. According to Condo-Russell model, [7, citation therein)] when the antiproton is captured, it replaces one of the electrons of the helium atom, where this Bohr orbit corresponds to such high quantum numbers for the antiproton which is 1,836 times heavier than electron. Antiproton then cascade with radiative transitions, the strongest of which being that of $(n,l) \rightarrow (n-1, l-1)$ which keeps the vibrational quantum number $v = n-l-1$, until it arrives at a short-lived state with fast Auger transition.

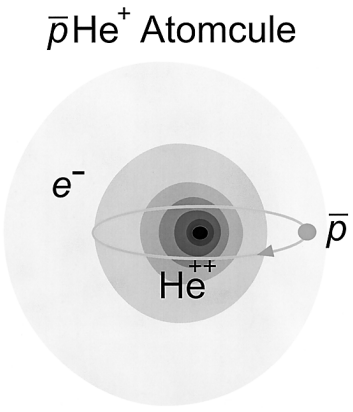

Fig. 4. A schematic picture of a $(\overline{p}He^+)^0$ atom, consisting of a helium nucleus (He^{++}), an antiproton ($\overline{p}$) and an electron (e^-). The $\overline{p}$ in a highly excited state moves round the helium nucleus along a classical orbit while the electron is in its $1s$ state, which is however slightly polarized by the repulsion of the $\overline{p}$ to the opposite side of the helium nucleus.

Our spectroscopic method was to irradiate the target with intense laser pulse to resonate the last transition in the cascade ladder and induce deexcitation to a short-lived state. Then the resonance was detected in the annihilation time spectrum as a sharp spike of the forced annihilation of antiprotons which followed fast Auger transition of $(\overline{p}He^+)^0$ to an unstable $(\overline{p}He^{++})^+$ state. With this "laser-induced annihilation spectroscopy" method,[7,8)] we have so far found 13 resonant transitions in the LEAR age, among high-n, high-l metastable states of the $(\overline{p}He^+)^0$ atoms. The observed transition energies showed excellent agreement with theoretical calculations and thus we have established the level structures of this exotic atom, as shown in Fig. 5. Especially, careful analysis of the observed density shift led to the deduction of the resonance frequencies for the three-body system unperturbed by collisions, which enabled us to set a severe constraint on the antiproton mass and charge, giving an important test of CPT invariance between proton and antiproton, as well as of bound-state QED theory.[9)]

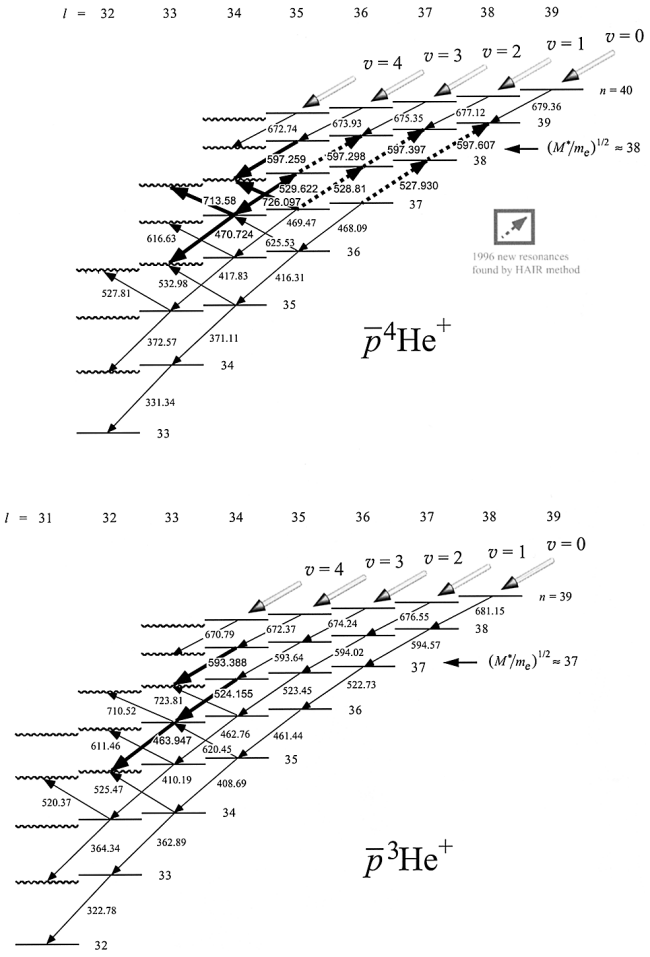

Fig. 5. Level diagrams of the metastable states of $\overline{p}^4He^+$ and $\overline{p}^3He^+$ atoms are shown with observed 13 laser-induced resonant transitions in thick arrows. States denoted by straight lines have long lifetimes of about a microsecond while those by zigzagged lines have shorter lifetimes than about 10 ns due to fast Auger transition to $(\overline{p}He^{++})^+$ states. The numbers for the observed transitions indicate experimental vacuum wavelengths, which may be subject to collisional density shift. Unobserved transitions are indicated with theoretically calculated transition wavelengths.

Also, time-resolved measurements have been performed by changing the timing of the laser pulse with respect to the antiprotonic atom formation. It clearly showed cascade feeding from upper states, and a systematic study combined with fitting of the data to a cascade model using rate equations enabled deduction of both the transition rate and population of each state. The result of the analysis showed that 10% of the metastable population sit in the cascade series $v = 3$ and 25% in $v = 2$, while the others should reside in $v = 1$ and 0 states.[10,11] We also can conclude that the antiprotons are captured in the $n \sim n_0 \approx 38$ states with a rather sharp distribution of n; a similarity can be seen with the case of electron transfer by highly charged ions (HCIs), as stated in the former section. This result, the first direct mapping of initial population of the states in the history of study of exotic atoms, gives clear information of atomic capture process of exotic particles.

Conclusion

In summary, we have performed time-resolved spectroscopy of high Rydberg states of highly charged ions ($Ar^{Q+}e^-$) and antiprotonic helium atoms ($(\overline{p}He^+)^0$). Although the object ions/atoms have quite different properties and the spectroscopic methods employed are also different, they have common similarity that one negative particle is in a highly excited Rydberg state with large quantum numbers n and l, and that the initial population can be deduced by fitting the time profile to the cascade model based on rate equations. The result of the analyses showed that the principal quantum number n has a rather sharp distribution around the value predicted by the classical over-barrier model for the HCI and by the Condo-Russell model for the antiprotonic atom. This success in mapping the population gives an important direct information on the processes of electron transfer and atomic capture of particles.

References

1) H. Winter: Europhys. Lett. **18**, 207 (1992).
2) F. Aumayr et al.: Phys. Rev. Lett. **71**, 1943 (1993).
3) S. Ninomiya et al.: Phys. Rev. Lett. **78**, 4557 (1997).
4) J. Burgdörfer et al.: Phys. Rev. A **44**, 5674 (1991).
5) Y. Morishita and H. A. Torii et al.: to be submitted.
6) ASACUSA experiment, http://www.cern.ch/ASACUSA/
7) N. Morita et al.: Phys. Rev. Lett. **72**, 1180 (1994).
8) H. A. Torii et al.: Nucl. Instrum. Methods Phys Res. A, **396**, 257 (1997).
9) H. A. Torii et al.: Phys. Rev. A **59**, 223 (1999).
10) R. S. Hayano et al.: Phys. Rev. Lett. **73**, 1485 (1994); Phys. Rev. Lett. **73**, 3181(E) (1994).
11) M. Hori and H. A. Torii et al.: Phys. Rev. A, **58**, 1612 (1998).